CASL-U-2014-0083-000

Power uprates
and plant life extension

Consortium for Advanced Simulation of LWRs

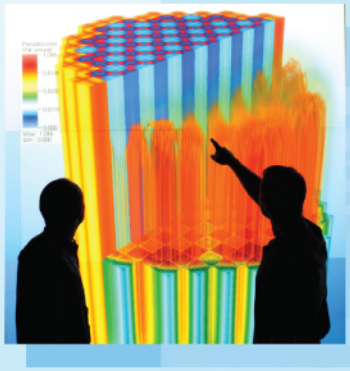

Engineering design
and analysis

L3: RTM.MCH.P6.02 Technical Note RNSD-00-000: Evaluating the Denovo SPN Discretization, Rev 1

Science-enabling
high performance
computing

Tom Evans
Oak Ridge National Laboratory

April 5, 2013

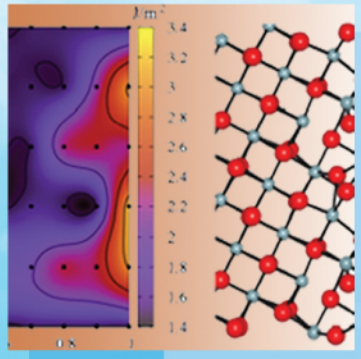

Fundamental science

Plant operational data

U.S. DEPARTMENT OF ENERGY | Nuclear Energy

OAK RIDGE NATIONAL LABORATORY
MANAGED BY UT-BATTELLE FOR THE DEPARTMENT OF ENERGY

Technical Note

Reactor and Nuclear Systems Division
Radiation Transport Group

From: Tom Evans, Steven Hamilton
Number: RNSD-00-000
Date: April 5, 2013

Subject: Evaluating the Denovo SP_N Discretization (Rev. 1)

Executive Summary

This document describes a preliminary assessment of the SP_N discretization in Denovo. Comparison to existing S_n discretizations is provided for three variants of CASL AMA Problem 2. Evaluation of the accuracy for both pin-resolved and pin-homogenized cross section processing options are studied.

1 Introduction

The Simplified P_N (SP_N) approximation is a three-dimensional extension of the plane-geometry P_N equations. It was originally proposed by Gelbard [1] who applied heuristic arguments to justify the approximation. Since that time, both asymptotic [2–4] and variational [5] analyses have verified Gelbard's approach. This note intends to start quantifying the accuracy of the SP_N discretization as implemented in Denovo in comparison to Denovo's traditional discrete ordinates discretizations. It is also anticipated that SP_N will not perform well when attempting to resolve interfaces between highly differing materials, so an assessment of the pincell homogenization strategies available in Scale are also necessary.

2 Methodology

The multigroup SP_Nequations are given by

$$-\frac{\partial}{\partial x_i}\left[\frac{n}{2n+1}(\mathbf{\Sigma}_{n-1}^{-1})\frac{\partial}{\partial x_i}\left(\frac{n-1}{2n-1}\Phi_{n-2}+\frac{n}{2n-1}\Phi_n\right)+\right.$$
$$\left.\frac{n+1}{2n+1}(\mathbf{\Sigma}_{n+1}^{-1})\frac{\partial}{\partial x_i}\left(\frac{n+1}{2n+3}\Phi_n+\frac{n+2}{2n+3}\Phi_{n+2}\right)\right]+\mathbf{\Sigma}_n\Phi_n=\frac{1}{k}\mathbf{F}\Phi_n\,,\quad n=0,2,\ldots,N\,,\tag{1}$$

where Φ_n indicates the nth angular moment of the angular flux, $\mathbf{\Sigma}_n=(\sigma-\sigma_{s,n})$, and $\mathbf{F}$ is the fission matrix. A standard transformation of the moment vectors is applied, i.e.

$$u_1=\phi_0+2\phi_2\,,\quad u_2=3\phi_2+4\phi_4\,,\quad u_3=5\phi_4+6\phi_6\,,\quad u_4=7\phi_6\,,\tag{2}$$

producing a system of equations that has a very diffusion-like appearance:

$$-\nabla\cdot\mathbb{D}_n\nabla\mathbb{U}_n+\sum_{m=1}^{4}\mathbb{A}_{nm}\mathbb{U}_m=\frac{1}{k}\sum_{m=1}^{4}\mathbb{F}_{nm}\mathbb{U}_{nm}\,,\quad n=1,2,3,4\,,\tag{3}$$

where the new solution vector, $\mathbb{U}$, represents the transformed flux moments.

In Denovo, a finite volume approach is used to spatially discretize the SP_N equations. Unlike traditional discrete ordinates transport discretizations, with SP_N it is possible to explicitly form the discretized matrices, offering numerous advantageous solver and preconditioning options. At the current time, Denovo is able to use either Arnoldi or generalized Davidson eigensolvers in combination with a wide variety of readily available solvers through Trilinos. In particular, Krylov subspace linear solvers in conjunction with the algebraic multigrid package, ML, have performed exceptionally well on the types of reactor problems studied so far.

3 Results

In order to assess the accuracy of the SPN discretization, three problems of increasing difficulty are proposed. These problems correspond to CASL AMA problems 2A, 2E, and 2H. The geometry for all three problems consists of a 17×17 array of fuel pins with 24 guide tubes and one instrumentation tube. The fuel pins consist of 3.1% enriched UO_2 fuel, a helium gap, Zircaloy 4 cladding, and natural water moderator with 1300 ppm soluble boron. In problem 2A, all guide tubes are filled with only water. For problem 2E, twelve of the guide tubes contain pyrex inserts. Problem 2H places B_4C control rods into all 24 guide tube locations; the strong absorption in the control rods causes this problem to be significantly more difficult than the other cases.

As a reference solution, we use the 2D bilinear discontinuous (BLD) spatial discretization of the discrete ordinates transport equation. A QR angular quadrature with eight azimuthal and six polar angles per octant is used for all BLD calculations. As mentioned previously, the SP_N equations in Denovo are discretized with a finite volume approach. For all problems, a problem-dependent energy collapse from a 252 group library to 23 energy groups is performed.

Two different methods of defining materials on the Denovo mesh are investigated. The first is a standard homogenization in which the material defined for each Denovo mesh cell is defined as a volume-weighted average of the true materials contained in that cell. We refer to this method as "resolved" because it reproduces the true problem in the limit as the mesh is refined. The second approach is a pincell homogenization approach which uses the XSDRN module in SCALE to perform a flux-weighted collapse to produce a single material in each pincell. Because this method does not approach the true geometry, even as the mesh is refined, we refer to this as the "homogenized" approach. In our current studies, the resolved BLD approach with a 64×64 mesh per pincell is used as the reference solution.

Figure 1 shows the effect of mesh refinement on the BLD and SP5 solutions on the computed eigenvalue and pin power distributions, respectively. At coarse meshes, resolved BLD and SP5 perform very similarly, but as the mesh is refined the BLD solution converges to the reference solution while the SP5 solution converges, but to a different solution than BLD. When cell homogenization is enabled, BLD and SP5 produce essentially identical results. Furthermore, the solution is essentially independent of the level of mesh refinement, due to the fact that the materials in Denovo mesh cells are not changing between mesh levels. As expected, the homogenized results do not converge to the reference solution, but the errors produced by this approach are quite small.

Figure 2 shows the same mesh refinement study for problem 2E. Although this is a more difficult problem, the same general trends from the previous problem are observed, with the exception that a slightly finer mesh is required to achieve a converged solution. Errors in the eigenvalue for the resolved SP5 solution are higher than is desirable (around 700 pcm from the reference solution), but the pin powers are fairly accurate for both resolved and homogenized SP5.

Problem 2H presents a much more significant challenge to the solvers than the previous cases, as exhibited in Figure 3. Achieving convergence requires a much finer mesh for the BLD discretization and the discrepancies between BLD and SP5 are much more noticeable than before. Homogenized SP5 produces a much better eigenvalue than resolved SP5, but even this solution differs from the reference case by over 1000 pcm. This result seems to indicate that in the presence of strong absorbers, the spatial homogenization of pincells independently is not an appropriate approach and a more robust strategy that accounts for the presence

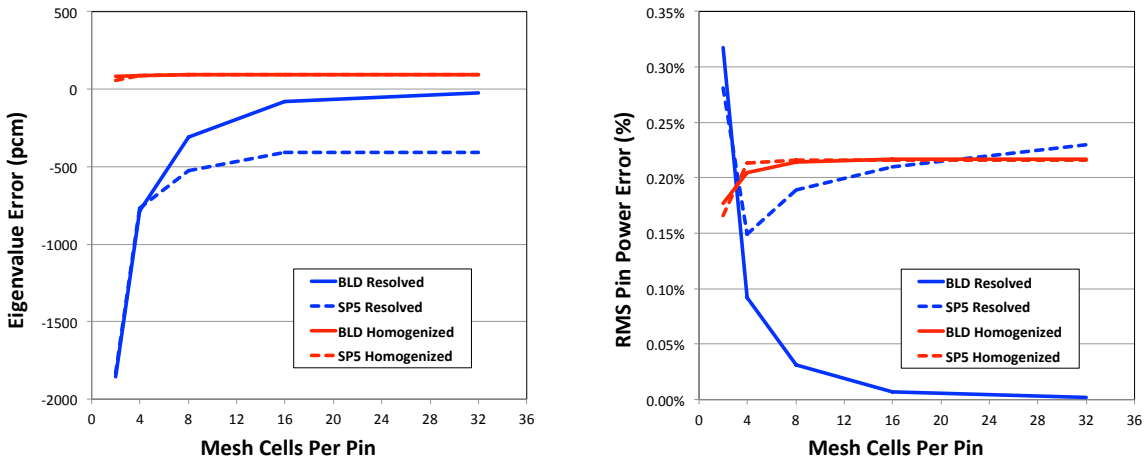

(a) Eigenvalue Convergence. (b) Pin Power Convergence.

Figure 1: Mesh Refinement Convergence for Problem 2A.

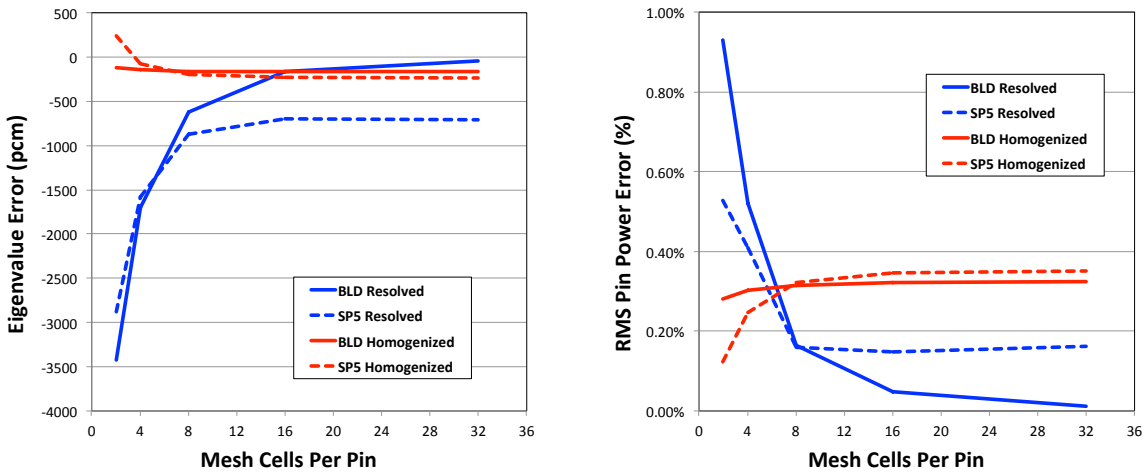

(a) Eigenvalue Convergence. (b) Pin Power Convergence.

Figure 2: Mesh Refinement Convergence for Problem 2E.

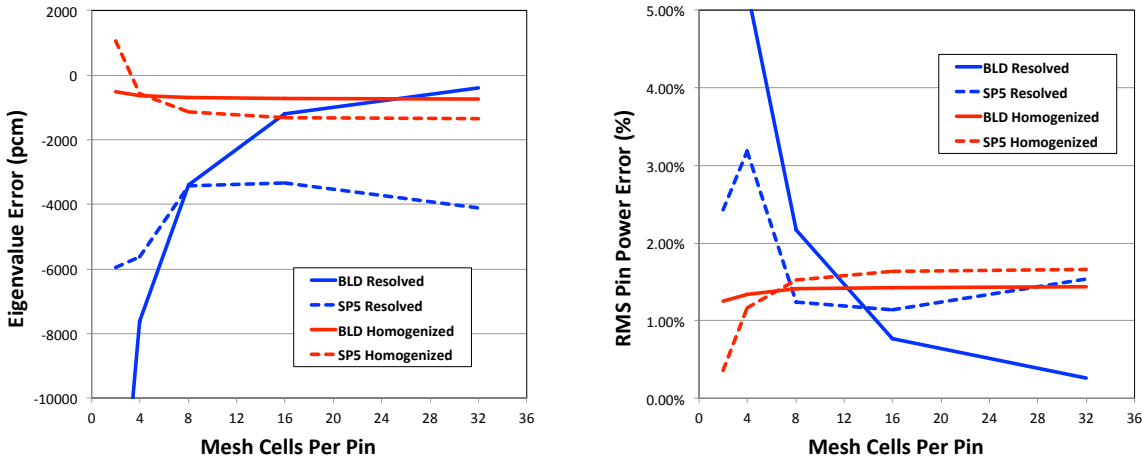

(a) Eigenvalue Convergence.

(b) Pin Power Convergence.

Figure 3: Mesh Refinement Convergence for Problem 2H.

of neighboring cells (possibly by performing a full detailed 2D calculation to produce a flux spectrum for homogenization) would be more accurate.

References

[1] E. Gelbard, "Application of the spherical harmonics to reactor problems," Tech. Rep. WAPD-BT-20, Westinghouse Atomic Power Department, Sept 1960.

[2] M. Frank, A. Klar, E. W. Larsen, and S. Yasuda, "Time-dependent simplified PN approximation to the equations of radiative transfer," *Journal of Computational Physics*, vol. 226, pp. 2289–2305, Oct. 2007.

[3] E. W. Larsen, G. Thömmes, A. Klar, M. Sead, and T. Götz, "Simplified PN Approximations to the Equations of Radiative Heat Transfer and Applications," *Journal of Computational Physics*, vol. 183, pp. 652–675, Dec. 2002.

[4] E. W. Larsen, J. E. Morel, and J. M. McGhee, "Asymptotic Derivation of the Multigroup P1 and Simplified PN Equations with Anisotropic Scattering," *Nuclear Science and Engineering*, vol. 123, pp. 328–342, 1996.

[5] P. S. Brantley and E. W. Larsen, "The Simplified P3 Approximation," *Nuclear Science and Engineering*, vol. 134, pp. 1–21, 2000.

Distribution

9te <9te@ornl.gov>

CAUTION

This document has not been given final patent clearance and is for internal use only. If this document is to be given public release, it must be cleared through the site Technical Information Office, which will see that the proper patent and technical information reviews are completed in accordance with the policies of Oak Ridge National Laboratory and UT-Battelle, LLC.

OAK RIDGE NATIONAL LABORATORY
MANAGED BY UT-BATTELLE FOR THE DEPARTMENT OF ENERGY

Technical Note

Reactor and Nuclear Systems Division
Radiation Transport Group

From: Tom Evans, Steven Hamilton
Number: RNSD-00-000
Date: April 5, 2013

Subject: Simplified P_N Methods in Denovo (Rev. 1)

Executive Summary

This document describes the Simplified P_N methods implemented in Denovo.

1 Introduction

The Simplified P_N (SP_N) approximation is a three-dimensional extension of the plane-geometry P_N equations. It was originally proposed by Gelbard [1] who applied heuristic arguments to justify the approximation. Since that time, both asymptotic [2–4] and variational [5] analyses have verified Gelbard's approach.

In this note we derive the SP_N equations using the original method of Gelbard. The presentation closely follows Refs. [4] and [6].

2 P_N Equations

We begin the derivation of the planar P_N equations from the steady-state, one-dimensional, monoenergetic transport equation,

$$\mu \frac{\partial \psi(x,\mu)}{\partial x} + \sigma(x)\psi(x,\mu) = \int_{4\pi} \sigma_{\mathrm{s}}(x, \hat{\mathbf{\Omega}} \cdot \hat{\mathbf{\Omega}}')\psi(x,\mathbf{\Omega}')\, d\mathbf{\Omega}' + \frac{q(x)}{4\pi} \,, \tag{1}$$

with boundary conditions,

$$\psi(x,\mu) = \psi_{\mathrm{b}}(x,\mu) \,, \quad x \in \partial V \,. \tag{2}$$

Here, the standard definitions hold:

$\psi(x,\mu)$	angular flux in particles·cm^{-2}·str^{-1}
$\sigma(x)$	total interaction cross section in cm^{-1}
$\sigma_{\mathrm{s}}(x, \hat{\mathbf{\Omega}} \cdot \hat{\mathbf{\Omega}}')$	scattering cross section through angle $\mu_0 = \hat{\mathbf{\Omega}} \cdot \hat{\mathbf{\Omega}}'$
$q(x)$	isotropic source in particles·cm^{-3}

The P_N equations are obtained by expanding the angular flux and scattering in Legendre polynomials (this requires spherical harmonics in two and three dimensions and non-cartesian geometry):

$$\psi(\mu) = \sum_{n=0}^{N} \frac{2n+1}{4\pi} \phi_n P_n(\mu) \,, \tag{3}$$

$$\sigma_{\mathrm{s}}(\mu_0) = \sum_{m=0}^{N} \frac{2m+1}{4\pi} \sigma_{\mathrm{s}m} P_m(\mu_0) \,, \tag{4}$$

where $\mu_0 = \hat{\mathbf{\Omega}} \cdot \hat{\mathbf{\Omega}}'$. In what follows we shall make use of the following properties of Legendre polynomials:

$$\int_{-1}^{1} P_n(\mu) P_m(\mu)\, d\mu = \frac{2}{2n+1}\delta_{nm}\,, \qquad \text{(orthogonality)} \tag{5}$$

$$(2n+1)\mu P_n(\mu) = (n+1)P_{n+1}(\mu) + nP_{n-1}(\mu)\,, \qquad \text{(recursion)} \tag{6}$$

$$P_l(\hat{\mathbf{\Omega}} \cdot \hat{\mathbf{\Omega}}') = \frac{4\pi}{2n+1} \sum_{m=-l}^{l} Y_{lm}(\mathbf{\Omega}) Y^*_{lm}(\mathbf{\Omega}')\,, \qquad \text{(addition theorem)} \tag{7}$$

Expanding the addition theorem we obtain

$$P_l(\hat{\mathbf{\Omega}} \cdot \hat{\mathbf{\Omega}}') = \frac{4\pi}{2n+1} \left[Y_{l0}(\mathbf{\Omega}) Y^*_{l0}(\mathbf{\Omega}') + \sum_{m=1}^{l} \left(Y_{l-m}(\mathbf{\Omega}) Y^*_{l-m}(\mathbf{\Omega}') + Y_{lm}(\mathbf{\Omega}) Y^*_{lm}(\mathbf{\Omega}') \right) \right]\,.$$

In planar geometry there is no azimuthal dependence and only $m = 0$ terms are required. Also, the spherical harmonics reduce to Legendre polynomials in planar geometry,

$$Y_{l0} = \sqrt{\frac{2l+1}{4\pi}} P_{l0} = \sqrt{\frac{2l+1}{4\pi}} P_l\,.$$

Combining these two equations, the addition theorem in planar geometry is

$$P_l(\hat{\mathbf{\Omega}} \cdot \hat{\mathbf{\Omega}}') = P_l(\mu_0) = P_l(\mu) P_l(\mu')\,. \tag{8}$$

From orthogonality we have

$$\phi_n = 2\pi \int_{-1}^{1} P_n(\mu) \psi(\mu)\, d\mu\,. \tag{9}$$

Applying the expansions in Eqs. (3) and (4) in Eq. (1) gives

$$\mu \frac{\partial}{\partial x} \left[\sum_n \frac{2n+1}{4\pi} \phi_n P_n(\mu) \right] + \sigma \sum_n \frac{2n+1}{4\pi} \phi_n P_n(\mu) = 2\pi \int_{-1}^{1} \sum_m \frac{2m+1}{4\pi} \sigma_{\mathrm{s}m} P_m(\mu_0) \sum_n \frac{2n+1}{4\pi} \phi_n P_n(\mu)\, d\mu' + \frac{q}{4\pi}\,, \tag{10}$$

where we have suppressed the x dependence. The P_N equations are obtained by multiplying by $P_m(\mu)$ and integrating by $\int_{-1}^{1} d\mu$. Equation (6) is used to remove μP_n from the derivative term. Equation (8) is used in the scattering expansion to remove the μ_0 dependence. Orthogonality is used to remove all the remaining Legendre polynomials. The resulting system of equations is

$$\frac{\partial}{\partial x} \left[\frac{n}{2n+1} \phi_{n-1} + \frac{n+1}{2n+1} \phi_{n+1} \right] + \Sigma_n \phi_n = q\delta_{n0}\,, \quad n = 0, 1, 2, \ldots, N\,, \tag{11}$$

where

$$\Sigma_n = \sigma - \sigma_{\mathrm{s}n}\,. \tag{12}$$

Equation (11) defines a system of $N+1$ equations that requires closure in order to deal with the ϕ_{n+1} term in the differential operator. The common method for closing the equations is to set this term to zero, $\phi_{N+1} = 0$. As an example, the P_3 equations are

$$\begin{aligned} \frac{\partial}{\partial x}(\phi_1) + \Sigma_0 \phi_0 &= q\,, \\ \frac{1}{3}\frac{\partial}{\partial x}(\phi_0 + 2\phi_2) + \Sigma_1 \phi_1 &= 0\,, \\ \frac{1}{5}\frac{\partial}{\partial x}(2\phi_1 + 3\phi_3) + \Sigma_2 \phi_2 &= 0\,, \\ \frac{1}{7}\frac{\partial}{\partial x}(3\phi_2) + \Sigma_3 \phi_3 &= 0\,. \end{aligned} \tag{13}$$

2.1 P_N Boundary Conditions

For this work we consider 3 types of boundary conditions:

- vacuum
- isotropic flux
- reflecting

For vacuum and isotropic flux we will employ the Marshak boundary conditions. The Marshak conditions approximately satisfy Eq. (2) at the boundary and are consistent with the P_N approximation. The generalized Marshak boundary condition is

$$2\pi \int_{\mu_{\rm in}} P_i(\mu)\psi(\mu)\,d\mu = 2\pi \int_{\mu_{\rm in}} P_i(\mu)\psi_{\rm b}(\mu)\,d\mu\,, \quad i = 1,3,5,\ldots,N\,. \tag{14}$$

Expanding ψ using Eq. (3) gives

$$2\pi \int_{\mu_{\rm in}} P_i(\mu) \sum_{n=0}^{N} \frac{2n+1}{4\pi}\phi_n P_n(\mu)\,d\mu = 2\pi \int_{\mu_{\rm in}} P_i(\mu)\psi_{\rm b}(\mu)\,d\mu\,, \quad i = 1,3,5,\ldots,N\,. \tag{15}$$

Equation (15) yields $(N+1)/2$ fully coupled equations at each boundary. Thus, it fully closes the $N+1$ P_N equations given in Eq. (11).

Once again, as an example we consider the P_3 equations. The Marshak conditions on the low boundary are derived using

$$2\pi \int_0^1 P_1(\mu) \sum_{n=0}^{3} \frac{2n+1}{4\pi}\phi_n P_n(\mu)\,d\mu = 2\pi \int_0^1 P_1(\mu)\psi_{\rm b}(\mu)\,d\mu \tag{16}$$

$$2\pi \int_0^1 P_3(\mu) \sum_{n=0}^{3} \frac{2n+1}{4\pi}\phi_n P_n(\mu)\,d\mu = 2\pi \int_0^1 P_3(\mu)\psi_{\rm b}(\mu)\,d\mu \tag{17}$$

Assuming an isotropic flux on the boundary,

$$\psi_{\rm b}(\mu) = \frac{\phi_{\rm b}}{4\pi}\,, \tag{18}$$

the P_3 Marshak boundary conditions are

$$\frac{1}{2}\phi_0 + \phi_1 + \frac{5}{8}\phi_2 = \frac{1}{2}\phi_{\rm b}\,, \tag{19}$$

$$-\frac{1}{8}\phi_0 + \frac{5}{8}\phi_2 + \phi_3 = -\frac{1}{8}\phi_{\rm b}\,. \tag{20}$$

As stated above, all of the moments are coupled in the boundary conditions. For a vacuum condition, $\phi_{\rm b} = 0$.

Reflecting boundary conditions are more straightforward. The only conditions that make physical sense in this case is to set all the odd moments to zero

$$\phi_i = 0\,, \quad i = 1,3,5,\ldots,N\,. \tag{21}$$

In the P_1 approximation this is equivalent to setting the current to zero at each boundary. From Eq. (9)

$$\phi_1 = 2\pi \int_{-1}^{1} \mu\psi(\mu)\,d\mu = J = 0\,. \tag{22}$$

This treatment also yields $(N+1)/2$ equations on each boundary and effectively closes the system.

We note that both of these boundary treatments contain asymmetric components when $N \in \{\text{even}\}$. Thus, we only consider odd sets of P_N (SP_N) equations.

3 SP_N Equations

As mentioned in § 1 the SP_N method is based on heuristic arguments; however, several studies have performed both asymptotic and variational analysis that have confirmed the original *ad hoc* approximations. In this note, we shall apply the heuristic approximation. The reader is directed towards Refs. [2–4] for more details on asymptotic derivations of the equations and Ref. [5] for a variational analysis of the SP_N equations.

In the notation that follows we will employ the Einstein Summation convention in which identical indices are implicitly summed over the range $1, \ldots, 3$,

$$a_i b_i = \sum_{i=1}^{3} a_i b_i = \mathbf{A} \cdot \mathbf{B} \,. \tag{23}$$

To form the SP_N equations the following substitutions are made in Eq. (11):

- $\frac{\partial}{\partial x} \to \frac{\partial}{\partial x_i}$,
- convert odd moments to $\phi_{n,i}$,
- use odd-order equations to remove odd moments from the even-order equations .

For boundary conditions a similar process holds except that $\pm\frac{\partial}{\partial x} \to n_i \frac{\partial}{\partial x_i}$, where $\hat{\mathbf{n}} = n_i \mathbf{i} + n_j \mathbf{j} + n_k \mathbf{k}$ is the outward normal at a boundary surface and $\mu \to |\hat{\mathbf{\Omega}} \cdot \hat{\mathbf{n}}|$. Using Eq. (11) and the rules described above, we have

$$\frac{\partial}{\partial x_i}\Big[\frac{n}{2n+1}\phi_{n-1,i} + \frac{n+1}{2n+1}\phi_{n+1,i}\Big] + \Sigma_n \phi_n = q\delta_{n0} \,, \qquad n = 0, 2, 4, \ldots, N \,, \tag{24}$$

$$\frac{\partial}{\partial x_i}\Big[\frac{n}{2n+1}\phi_{n-1} + \frac{n+1}{2n+1}\phi_{n+1}\Big] + \Sigma_n \phi_{n,i} = 0 \,, \qquad n = 1, 3, 5, \ldots, N \,. \tag{25}$$

Using Eq. (25) to solve for the odd moments gives

$$\phi_{n,i} = -\frac{1}{\Sigma_n}\frac{\partial}{\partial x_i}\Big[\frac{n}{2n+1}\phi_{n-1} + \frac{n+1}{2n+1}\phi_{n+1}\Big] \,. \tag{26}$$

Substituting Eq. (26) into Eq. (24) gives

$$\begin{aligned} -\frac{\partial}{\partial x_i}\Bigg[\frac{n}{2n+1}\frac{1}{\Sigma_{n-1}}\frac{\partial}{\partial x_i}\Big(\frac{n-1}{2n-1}\phi_{n-2} + \frac{n}{2n-1}\phi_n\Big) + \\ \frac{n+1}{2n+1}\frac{1}{\Sigma_{n+1}}\frac{\partial}{\partial x_i}\Big(\frac{n+1}{2n+3}\phi_n + \frac{n+2}{2n+3}\phi_{n+2}\Big)\Bigg] + \\ \Sigma_n \phi_n = q\delta_{n0} \,, \quad m = 0, 2, \ldots, N \,. \end{aligned} \tag{27}$$

Equation (27) gives the $(N+1)/2$ SP_N equations. Each equation has a diffusion-like form. The boundary conditions are derived in the same manner, and Eq. (26) is used to remove the odd moments.

3.1 SP_7 Equations

In all that follows, we will use the SP_7 equations as a model system. From Eq. (27) the four $((N+1)/2)$ SP_7 equations are

$$\begin{aligned} -\nabla \cdot \frac{1}{3\Sigma_1}\nabla(\phi_0 + 2\phi_2) + \Sigma_0\phi_0 &= q \,, \\ -\nabla \cdot \Big[\frac{2}{15\Sigma_1}\nabla(\phi_0 + 2\phi_2) + \frac{3}{35\Sigma_3}\nabla(3\phi_2 + 4\phi_4)\Big] + \Sigma_2\phi_2 &= 0 \,, \\ -\nabla \cdot \Big[\frac{4}{63\Sigma_3}\nabla(3\phi_2 + 4\phi_4) + \frac{5}{99\Sigma_5}\nabla(5\phi_4 + 6\phi_6)\Big] + \Sigma_4\phi_4 &= 0 \,, \\ -\nabla \cdot \Big[\frac{6}{143\Sigma_5}\nabla(5\phi_4 + 6\phi_6) + \frac{7}{195\Sigma_7}\nabla(7\phi_6)\Big] + \Sigma_6\phi_6 &= 0 \,, \end{aligned} \tag{28}$$

where we have converted $\frac{\partial}{\partial x_i} a_i = \nabla \cdot \mathbf{a}$. The diffusion-like nature of Eqs. (28) is more easily understood by making the following change of variables:

$$u_1 = \phi_0 + 2\phi_2 \,, \quad u_2 = 3\phi_2 + 4\phi_4 \,, \quad u_3 = 5\phi_4 + 6\phi_6 \,, \quad u_4 = 7\phi_6 \,. \tag{29}$$

The inverse of this system is

$$\phi_0 = u_1 - \frac{2}{3}u_2 + \frac{8}{15}u_3 - \frac{16}{35}u_4 \,, \quad \phi_2 = \frac{1}{3}u_2 - \frac{4}{15}u_3 + \frac{8}{35}u_4 \,, \quad \phi_4 = \frac{1}{5}u_3 - \frac{6}{35}u_4 \,, \quad \phi_6 = \frac{1}{7}u_4 \,, \tag{30}$$

Using Eqs. (29) and (30) in Eq. (28) gives the following system of equations in terms of ,

$$-\nabla \cdot D_n \nabla u_n + \sum_{m=1}^{4} A_{nm} u_m = Q_n \,, \quad n = 1, 2, 3, 4 \,, \tag{31}$$

where

$$\mathbf{u} = \begin{pmatrix} u_1 & u_2 & u_3 & u_4 \end{pmatrix}^T \,, \tag{32}$$

$$\mathbf{D} = \begin{pmatrix} \frac{1}{3\Sigma_1} & \frac{1}{7\Sigma_3} & \frac{1}{11\Sigma_5} & \frac{1}{15\Sigma_7} \end{pmatrix}^T \,, \tag{33}$$

$$\mathbf{Q} = \begin{pmatrix} q & -\frac{2}{3}q & \frac{8}{15}q & -\frac{16}{35}q \end{pmatrix}^T \,, \tag{34}$$

and

$$\mathbf{A} = \begin{pmatrix} (\Sigma_0) & (-\frac{2}{3}\Sigma_0) & (\frac{8}{15}\Sigma_0) & (-\frac{16}{35}\Sigma_0) \\ (-\frac{2}{3}\Sigma_0) & (\frac{4}{9}\Sigma_0 + \frac{5}{9}\Sigma_2) & (-\frac{16}{45}\Sigma_0 - \frac{4}{9}\Sigma_2) & (\frac{32}{105}\Sigma_0 + \frac{8}{21}\Sigma_2) \\ (\frac{8}{15}\Sigma_0) & (-\frac{16}{45}\Sigma_0 - \frac{4}{9}\Sigma_2) & (\frac{64}{225}\Sigma_0 + \frac{16}{45}\Sigma_2 + \frac{9}{25}\Sigma_4) & (-\frac{128}{525}\Sigma_0 - \frac{32}{105}\Sigma_2 - \frac{54}{175}\Sigma_4) \\ (-\frac{16}{35}\Sigma_0) & (\frac{32}{105}\Sigma_0 + \frac{8}{21}\Sigma_2) & (-\frac{128}{525}\Sigma_0 - \frac{32}{105}\Sigma_2 - \frac{54}{175}\Sigma_4) & (\frac{256}{1225}\Sigma_0 + \frac{64}{245}\Sigma_2 + \frac{324}{1225}\Sigma_4 + \frac{13}{49}\Sigma_6) \end{pmatrix} . \tag{35}$$

Equation (28) are the SP_7 equations that we will use in the remainder of this paper. This system reduces to the SP_1 (diffusion) equation by setting $\phi_2 = \phi_4 = \phi_6 = 0$,

$$-\nabla \cdot \frac{1}{3\Sigma_1} \nabla \phi_0 + \Sigma_0 \phi_0 = q \,. \tag{36}$$

Equivalently, the SP_3 equations are obtained by setting $\phi_4 = \phi_6 = 0$ and the SP_5 equations result from setting $\phi_6 = 0$.

The P_7 Marshak boundary conditions are obtained by carrying out the integrations in Eq. (15) using the isotropic boundary flux condition in Eq. (18):

$$\begin{aligned} \frac{1}{2}\phi_0 + \phi_1 + \frac{5}{8}\phi_2 - \frac{3}{16}\phi_4 + \frac{13}{128}\phi_6 &= \frac{1}{2}\phi_\mathrm{b} \,, \\ -\frac{1}{8}\phi_0 + \frac{5}{8}\phi_2 + \phi_3 + \frac{81}{128}\phi_4 - \frac{13}{64}\phi_6 &= -\frac{1}{8}\phi_\mathrm{b} \,, \\ \frac{1}{16}\phi_0 - \frac{25}{128}\phi_2 + \frac{81}{128}\phi_4 + \phi_5 + \frac{325}{512}\phi_6 &= \frac{1}{16}\phi_\mathrm{b} \,, \\ -\frac{5}{128}\phi_0 + \frac{7}{64}\phi_2 - \frac{105}{512}\phi_4 + \frac{325}{512}\phi_6 + \phi_7 &= -\frac{5}{128}\phi_\mathrm{b} \,. \end{aligned} \tag{37}$$

Using Eq. (11) to remove the odd-moments ($\{\phi_1, \phi_3, \phi_5, \phi_7\}$) from Eq. (37) and applying Eqs. (29) and (30) and the SP_N boundary approximation,

$$\pm \frac{\partial}{\partial x} \to \hat{\mathbf{n}} \cdot \nabla \,,$$

gives the SP_7 boundary conditions,

$$\hat{\mathbf{n}} \cdot D_n \nabla u_n + \sum_{m=1}^{4} B_{nm} u_m = s_n \ , \quad n = 1, 2, 3, 4 \ . \tag{38}$$

Here, u_n and D_n are defined in Eqs. (32) and (33). The right-hand side source, s_n is defined

$$\mathbf{s} = \begin{pmatrix} \frac{1}{2}\phi_{\mathrm{b}} & -\frac{1}{8}\phi_{\mathrm{b}} & \frac{1}{16}\phi_{\mathrm{b}} & -\frac{5}{128}\phi_{\mathrm{b}} \end{pmatrix}^T \ , \tag{39}$$

and $\mathbf{B}$ is

$$\mathbf{B} = \begin{pmatrix} \frac{1}{2} & -\frac{1}{8} & \frac{1}{16} & -\frac{5}{128} \\ -\frac{1}{8} & \frac{7}{24} & -\frac{41}{384} & \frac{1}{16} \\ \frac{1}{16} & -\frac{41}{384} & \frac{407}{1920} & -\frac{233}{2560} \\ -\frac{5}{128} & \frac{1}{16} & -\frac{233}{2560} & \frac{3023}{17920} \end{pmatrix} \ . \tag{40}$$

Performing the same truncation as above for the SP_1 equations, the boundary conditions become

$$\frac{1}{4}\phi_0 - \frac{1}{2}\hat{\mathbf{n}} \cdot \mathbf{J} = j^{\mathrm{in}} \ , \tag{41}$$

where

$$j^{\mathrm{in}} = 2\pi \int_0^1 \mu \frac{\phi_{\mathrm{b}}}{4\pi} \, d\mu = \frac{\phi_{\mathrm{b}}}{4} \ ,$$

and

$$\mathbf{J}_n = -D_n \nabla u_n \ . \tag{42}$$

This is the standard three-dimensional diffusion Marshak boundary condition, and Eq. (42) is Fick's Law.

The P_N boundary conditions for reflecting surfaces are given in Eq. (21). Applying the SP_N approximation to these boundary conditions yields

$$\nabla u_n = 0 \ , \quad n = 1, 2, 3, 4 \ . \tag{43}$$

This implies that $\hat{\mathbf{n}} \cdot \mathbf{J} = 0$ on the boundaries.

In summary, the SP_7 equations are given in Eq. (31) and yield $(N+1)/2$ second-order equations. The SP_7 Marshak boundary conditions are given in Eq. (38) for vacuum and isotropic boundary sources. Equation (43) gives reflecting boundary conditions. Each boundary condition yields $(N+1)/2$ first-order (Robin) conditions that closes the system of SP_N equations.

4 Finite Volume Discretization

The general form for the SP_7 equations is given in Eq. (31) with Marshak boundary conditions defined in Eq. (38) and reflecting boundary conditions given by Eq. (43). Applying Fick's Law (Eq. (42)) to Eq. (31) gives

$$\nabla \cdot \mathbf{J}_n + \sum_{m=1}^{4} A_{nm} u_m = Q_n \ , \quad n = 1, 2, 3, 4 \ . \tag{44}$$

To begin the finite-volume spatial discretization, consider the three-dimensional, orthogonal, Cartesian mesh cell illustrated in Fig. 1. Integrating over volume yields, with piece-wise constant A_{nm},

$$\int_V \nabla \cdot \mathbf{J}_n \, dV + \sum_{m=1}^{4} A_{nm,ijk} u_{m,ijk} V_{ijk} = Q_{n,ijk} V_{ijk} \ , \tag{45}$$

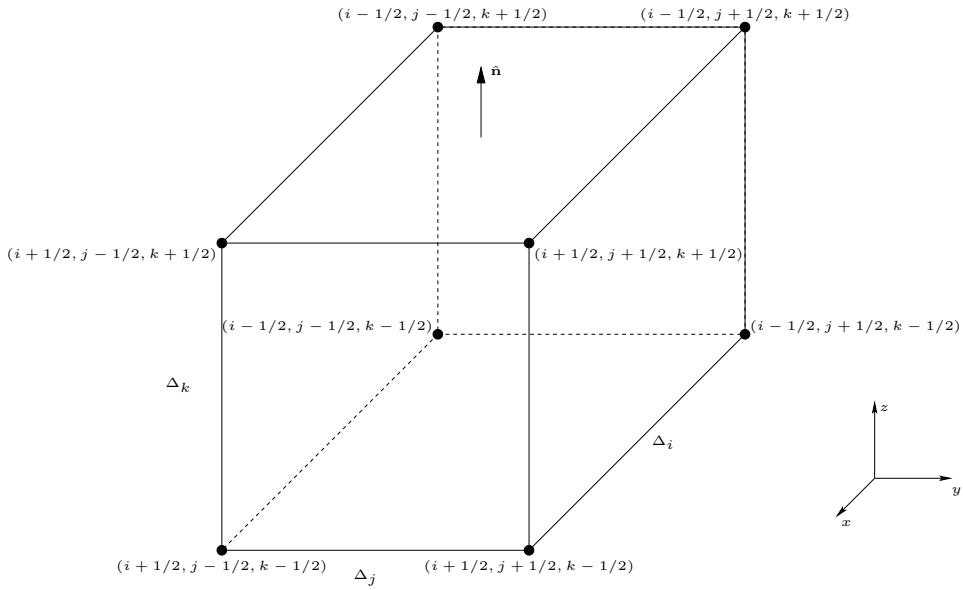

Figure 1: Three-dimensional, Cartesian mesh cell.

where

$$u_{n,ijk} = \frac{1}{V_{ijk}} \int_V u_n \, dV \; , \tag{46}$$

and

$$V_{ijk} = \Delta_i \Delta_j \Delta_k \; . \tag{47}$$

The Divergence Theorem gives[1]

$$\int_V \nabla \cdot \mathbf{J}_n \, dV = \oint \hat{\mathbf{n}} \cdot \mathbf{J}_n \, dA = \sum_{f=1}^{6} \hat{\mathbf{n}}_f \cdot \mathbf{J}_{n,f} A_f \; , \tag{48}$$

where f is the index over faces such that $f \in \{1, ..., 6\}$ as illustrated in Fig. 1. Applying these terms to Eq. (45) gives the discrete balance equation for Eq. (44):

$$(J_{n,i+1/2} - J_{n,i-1/2})\Delta_j \Delta_k + (J_{n,j+1/2} - J_{n,j-1/2})\Delta_i \Delta_k + (J_{n,k+1/2} - J_{n,k-1/2})\Delta_i \Delta_j + \sum_{m=1}^{4} A_{nm,ijk} u_{m,ijk} V_{ijk} = Q_{n,ijk} V_{ijk} \; . \tag{49}$$

Here, we have written the face-edge currents with suppressed subscripts as follows:

$$J_{n,i\pm1/2\,jk} \rightarrow J_{n,i\pm1/2} \; ,$$
$$J_{n,i\,j\pm1/2\,k} \rightarrow J_{n,j\pm1/2} \; ,$$
$$J_{n,ij\,k\pm1/2} \rightarrow J_{n,k\pm1/2} \; .$$

The same convention will be applied to all face-edge quantities.

[1]Note that $\hat{\mathbf{n}} = n_i \mathbf{i} + n_j \mathbf{j} + n_k \mathbf{k}$ is the outward normal whereas the $_n$ subscript indicates the index of the moment equation, $n \in \{1, 2, 3, 4\}$.

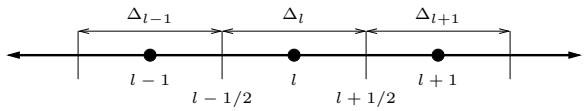

Figure 2: Difference mesh along a single direction $l \in \{i, j, k\}$.

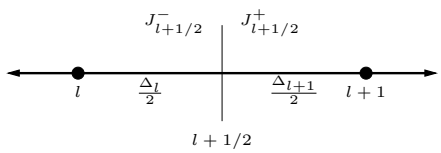

Figure 3: Illustration of continuous current at inter-cell boundaries.

Applying second-order differencing to Fick's Law, Eq. (42), in each direction as illustrated in Fig. 2 gives

$$\begin{aligned} J_{n,l+1/2} &= -D_{n,l+1/2}\frac{u_{n,l+1}-u_{n,l}}{\Delta_{l+1/2}}\,, \\ J_{n,l-1/2} &= -D_{n,l-1/2}\frac{u_{n,l}-u_{n,l-1}}{\Delta_{l-1/2}}\,, \end{aligned} \tag{50}$$

where

$$\begin{aligned} \Delta_{l+1/2} &= \frac{\Delta_l+\Delta_{l+1}}{2}\,, \\ \Delta_{l-1/2} &= \frac{\Delta_l+\Delta_{l-1}}{2}\,, \end{aligned} \tag{51}$$

for $l = i, j, k$. The true current is the first moment of the angular flux and is formally obtained only in the case of SP_1. However; these equations represent *effective* currents that are mathematically indistinguishable from the true current in higher order SP_N expansions. Plugging Eq. (50) into Eq. (49) gives

$$\begin{aligned} &\frac{D_{n,i+1/2}}{\Delta_{i+1/2}}(u_{n,ijk}-u_{n,i+1\,jk})\Delta_j\Delta_k+\frac{D_{n,i-1/2}}{\Delta_{i-1/2}}(u_{n,ijk}-u_{n,i-1\,jk})\Delta_j\Delta_k+ \\ &\qquad \frac{D_{n,j+1/2}}{\Delta_{j+1/2}}(u_{n,ijk}-u_{n,i\,j+1\,k})\Delta_i\Delta_k+\frac{D_{n,j-1/2}}{\Delta_{j-1/2}}(u_{n,ijk}-u_{n,i\,j-1\,k})\Delta_i\Delta_k+ \\ &\qquad \frac{D_{n,k+1/2}}{\Delta_{k+1/2}}(u_{n,ijk}-u_{n,ij\,k+1})\Delta_i\Delta_j+\frac{D_{n,k-1/2}}{\Delta_{k-1/2}}(u_{n,ijk}-u_{n,ij\,k-1})\Delta_i\Delta_j+ \\ &\qquad\qquad \sum_{m=1}^{4}A_{nm,ijk}u_{m,ijk}V_{ijk}=Q_{n,ijk}V_{ijk}\,. \end{aligned} \tag{52}$$

In order to complete the derivation of the discrete equations, the cell-edge diffusion coefficients must be calculated. To make the method consistent, the scalar and first derivatives must by continuous at inter-cell boundaries. This condition implies that the effective current, $\mathbf{J}$, is continuous across the boundary as illustrated in Fig. 3. Applying continuity of current at the $l \pm 1/2$ boundaries requires

$$J^-_{n,l\pm1/2} = J^+_{n,l\pm1/2}\,,$$

which results in the following conditions

$$-2D_{n,l}\frac{u_{n,l+1/2}-u_{n,l}}{\Delta_l} = -2D_{n,l+1}\frac{u_{n,l+1}-u_{n,l+1/2}}{\Delta_{l+1}}\ , \tag{53}$$

$$-2D_{n,l-1}\frac{u_{n,l-1/2}-u_{n,l-1}}{\Delta_{l-1}} = -2D_{n,l}\frac{u_{n,l}-u_{n,l-1/2}}{\Delta_l}\ . \tag{54}$$

Solving for $u_{n,l\pm1/2}$ gives

$$u_{n,l+1/2} = \frac{D_{n,l+1}\Delta_l u_{n,l+1} + D_{n,l}\Delta_{l+1}u_{n,l}}{D_{n,l}\Delta_{l+1} + D_{n,l+1}\Delta_l}\ , \tag{55}$$

$$u_{n,l-1/2} = \frac{D_{n,l}\Delta_{l-1} u_{n,l} + D_{n,l-1}\Delta_l u_{n,l-1}}{D_{n,l-1}\Delta_l + D_{n,l}\Delta_{l-1}}\ . \tag{56}$$

Plugging these face-edge fluxes into $J^+_{n,l\pm1/2}$ and setting the resulting face-edge currents equal to the discrete currents defined in Eq. (50) yields expressions for the face-edge diffusion coefficients:

$$\begin{aligned} D_{n,l+1/2} &= \frac{D_{n,l+1}D_{n,l}\Delta_l + D_{n,l}D_{n,l+1}\Delta_{l+1}}{D_{n,l}\Delta_{l+1} + D_{n,l+1}\Delta_l}\ , \\ D_{n,l-1/2} &= \frac{D_{n,l}D_{n,l-1}\Delta_l + D_{n,l}D_{n,l-1}\Delta_{l-1}}{D_{n,l-1}\Delta_l + D_{n,l}\Delta_{l-1}}\ , \\ l &= i,j,k\ . \end{aligned} \tag{57}$$

Having defined face-edge diffusion coefficients that preserves continuity of the first derivative (effective) at inter-cell boundaries, the complete discrete SP_N equations can be formulated. Plugging Eq. (57) into Eq. (52) gives

$$\begin{aligned} &-C^+_{n,i}u_{n,i+1\,jk} - C^-_{n,i}u_{n,i-1\,jk} - C^+_{n,j}u_{n,i\,j+1\,k} - C^-_{n,j}u_{n,i\,j-1\,k} - C^+_{n,k}u_{n,ij\,k+1} - C^-_{n,k}u_{n,ij\,k-1} - \\ &\sum_{m=1}^{4}\left[A_{nm,ijk} + (C^+_{m,i} + C^-_{m,i} + C^+_{m,j} + C^-_{m,j} + C^+_{m,k} + C^-_{m,k})\delta_{nm}\right]u_{m,ijk} = Q_{n,ijk}\ , \quad n = 1,2,3,4\ . \end{aligned} \tag{58}$$

The matrix $\mathbf{C}$ couples the angular moments, $\mathbf{u}$, in space and is defined

$$\begin{aligned} C^+_{n,l} &= \frac{2D_{n,l+1}D_{n,l}}{\Delta_l(D_{n,l}\Delta_{l+1} + D_{n,l+1}\Delta_l)}\ , \\ C^-_{n,l} &= \frac{2D_{n,l}D_{n,l-1}}{\Delta_l(D_{n,l-1}\Delta_l + D_{n,l}\Delta_{l-1})}\ , \\ l &= i,j,k\ . \end{aligned} \tag{59}$$

Equation (58) is the discrete SP_7 equation. For all $N > 1$ the equation couples all of the angular moments through $\mathbf{A}$.

All that remains to complete the discrete description of the problem is to incorporate the boundary conditions given in Eqs. (38) and (43). Using Fick's Law (42) in Eq. (38) gives

$$-\hat{\mathbf{n}}\cdot\mathbf{J}_n + \sum_{m=1}^{4} B_{nm}u_m = s_n\ , \quad n = 1,2,3,4\ . \tag{60}$$

At the low and high boundaries this yields

$$J_{n,1/2} = s_{n,1} - \sum_{m=1}^{4} B_{nm}u_{m,1/2}\ , \qquad \text{Low Boundary}\ , \tag{61}$$

$$J_{n,L+1/2} = \sum_{m=1}^{4} B_{nm}u_{m,L+1/2} - s_{n,L}\ , \qquad \text{High Boundary}\ , \tag{62}$$

where $l \in [1, L]$ is the range of cells in each direction such that $l = 1/2$ is the low-edge boundary and $l = L + 1/2$ is the high-edge boundary. Also, we have suppressed the complimentary directional subscripts. As before Eq. (42) is discretized at the boundaries yielding

$$J_{n,1/2} = -2D_{n,1}\frac{u_{n,1} - u_{n,1/2}}{\Delta_1} \,, \tag{63}$$

$$J_{n,L+1/2} = -2D_{n,L}\frac{u_{n,L+1/2} - u_{n,L}}{\Delta_L} \,. \tag{64}$$

Because all of the moments are coupled at the boundary, it is necessary to include the edge-fluxes in the solution vector. Thus, we require additional equations at the boundary to close the system. Equating the current equations at the low and high boundaries gives

$$\sum_{m=1}^{4}\Big(B_{nm} + \frac{2D_{n,1}}{\Delta_1}\delta_{nm}\Big)u_{m,1/2} - \frac{2D_{n,1}}{\Delta_1}u_{n,1} = s_n \,, \qquad \text{Low Boundary} \,, \tag{65}$$

$$\sum_{m=1}^{4}\Big(B_{nm} + \frac{2D_{n,L}}{\Delta_L}\delta_{nm}\Big)u_{m,L+1/2} - \frac{2D_{n,L}}{\Delta_L}u_{n,L} = s_n \,, \qquad \text{High Boundary} \,. \tag{66}$$

For boundaries described by Marshak conditions, Eqs. (63) and (64) are used in Eq. (49) for the edge-currents and Eqs. (65) and (66) provide the additional equations for the edge-fluxes.

Reflecting boundary conditions for the SP_7 equations are given in Eq. (43). These imply that

$$J_{n,1/2} = 0 \,, \tag{67}$$

$$J_{n,L+1/2} = 0 \,. \tag{68}$$

These boundary currents are used to close Eq. (49) on reflecting boundary faces.

5 Multigroup SP_N

The derivation of the SP_7 equations and the accompanying finite volume discretization has been for energy-independent or, equivalently, one-group problems. To include energy dependence we apply the multigroup approximation [7] to Eq. (1):,

$$\mu\frac{\partial\psi^g(x,\mu)}{\partial x} + \sigma^g(x)\psi^g(x,\mu) = \sum_{g'=0}^{G}\int_{4\pi}\sigma_{\mathrm{s}}^{gg'}(x,\hat{\mathbf{\Omega}}\cdot\hat{\mathbf{\Omega}}')\psi^{g'}(x,\mathbf{\Omega}')\,d\mathbf{\Omega}' + \frac{q^g(x)}{4\pi} \,, \tag{69}$$

where $g = 0, 1, \ldots, G$ is the energy group index for N_g total groups. Applying the P_N method described in § 2 and then making the SP_N approximation gives multigroup analogs of Eqs. (24) and (25)

$$\frac{\partial}{\partial x_i}\Big[\frac{n}{2n+1}\phi^g_{n-1,i} + \frac{n+1}{2n+1}\phi^g_{n+1,i}\Big] + \sum_{g'}(\sigma^g\delta_{gg'} - \sigma_{\mathrm{s}n}^{gg'})\phi_n^{g'} = q^g\delta_{n0} \,, \qquad n = 0, 2, 4, \ldots, N \,, \tag{70}$$

$$\frac{\partial}{\partial x_i}\Big[\frac{n}{2n+1}\phi^g_{n-1} + \frac{n+1}{2n+1}\phi^g_{n+1}\Big] + \sum_{g'}(\sigma^g\delta_{gg'} - \sigma_{\mathrm{s}n}^{gg'})\phi_{n,i}^{g'} = 0 \,, \qquad n = 1, 3, 5, \ldots, N \,. \tag{71}$$

Defining

$$\Phi_n = \begin{pmatrix}\phi_n^0 & \phi_n^1 & \ldots & \phi_n^G\end{pmatrix}^T \,, \tag{72}$$

$$\Phi_{n,i} = \begin{pmatrix}\phi_{n,i}^0 & \phi_{n,i}^1 & \ldots & \phi_{n,i}^G\end{pmatrix}^T \,, \tag{73}$$

$$\mathbf{q} = \begin{pmatrix}q^0 & q^1 & \ldots & q^G\end{pmatrix}^T \,, \tag{74}$$

and

$$\mathbf{\Sigma}_n = \begin{pmatrix} (\sigma^0 - \sigma_{sn}^{00}) & -\sigma_{sn}^{01} & \dots & -\sigma_{sn}^{0G} \\ -\sigma_{sn}^{10} & (\sigma^1 - \sigma_{sn}^{11}) & \dots & -\sigma_{sn}^{1G} \\ \vdots & \vdots & \ddots & \vdots \\ -\sigma_{sn}^{G0} & -\sigma_{sn}^{G1} & \dots & (\sigma^G - \sigma_{sn}^{GG}) \end{pmatrix} . \tag{75}$$

Thus, Φ_n and $\Phi_{n,i}$ are $(N_g \times 1)$ vectors and $\mathbf{\Sigma}$ is a $(N_g \times N_g)$ matrix. Solving Eq. (71) for $\Phi_{n,i}$ and plugging into Eq. (70) gives the multigroup SP_N equations

$$-\frac{\partial}{\partial x_i}\left[\frac{n}{2n+1}(\mathbf{\Sigma}_{n-1}^{-1})\frac{\partial}{\partial x_i}\left(\frac{n-1}{2n-1}\Phi_{n-2} + \frac{n}{2n-1}\Phi_n\right) + \frac{n+1}{2n+1}(\mathbf{\Sigma}_{n+1}^{-1})\frac{\partial}{\partial x_i}\left(\frac{n+1}{2n+3}\Phi_n + \frac{n+2}{2n+3}\Phi_{n+2}\right)\right] + \mathbf{\Sigma}_n\Phi_n = \mathbf{q}\delta_{n0} , \quad m = 0, 2, \dots, N . \tag{76}$$

Equation (76) is identical in form to the monoenergetic SP_N equations in (27) with the exception that unknowns are vectors of length N_g and the cross sections are $(N_g \times N_g)$ matrices.

Now, we make the same algebraic transforms as Eqs. (29) and (30) to define $\mathbb{U}_n$,

$$\mathbb{U}_1 = \Phi_0 + 2\Phi_2 , \quad \mathbb{U}_2 = 3\Phi_2 + 4\Phi_4 , \quad \mathbb{U}_3 = 5\Phi_4 + 6\Phi_6 , \quad \mathbb{U}_4 = 7\Phi_6 . \tag{77}$$

The effective diffusion coefficients in the multigroup problem are $(N_g \times N_g)$ matrices and are defined

$$\mathbb{D}_1 = \frac{1}{3}\mathbf{\Sigma}_1^{-1} , \quad \mathbb{D}_2 = \frac{1}{7}\mathbf{\Sigma}_3^{-1} , \quad \mathbb{D}_3 = \frac{1}{11}\mathbf{\Sigma}_5^{-1} , \quad \mathbb{D}_4 = \frac{1}{15}\mathbf{\Sigma}_7^{-1} . \tag{78}$$

The source is a $(N_g \times 1)$ column vector for each moment,

$$\mathbb{Q}_1 = \mathbf{q} , \quad \mathbb{Q}_2 = -\frac{2}{3}\mathbf{q} , \quad \mathbb{Q}_3 = \frac{8}{15}\mathbf{q} , \quad \mathbb{Q}_4 = -\frac{16}{35}\mathbf{q} . \tag{79}$$

The resulting multigroup SP_7 equations are

$$-\nabla \cdot \mathbb{D}_n \nabla \mathbb{U}_n + \sum_{m=1}^{4} \mathbb{A}_{nm}\mathbb{U}_m = \mathbb{Q}_n , \quad n = 1, 2, 3, 4 , \tag{80}$$

where each $\mathbb{A}_{nm}$ is a $(N_g \times N_g)$ block matrix. The effective Fick's Law for these equations is

$$\mathbb{J}_n = -\mathbb{D}_n \nabla \mathbb{U}_n , \tag{81}$$

where $\mathbb{J}$ is a $(N_g \times 1)$ vector.

Applying the same discretization from § 4 to Eq. (80) gives the multigroup equivalent of Eq. (49):

$$(\mathbb{J}_{n,i+1/2} - \mathbb{J}_{n,i-1/2})\Delta_j\Delta_k + (\mathbb{J}_{n,j+1/2} - \mathbb{J}_{n,j-1/2})\Delta_i\Delta_k + (\mathbb{J}_{n,k+1/2} - \mathbb{J}_{n,k-1/2})\Delta_i\Delta_j + \sum_{m=1}^{4} \mathbb{A}_{nm,ijk}\mathbb{U}_{m,ijk}V_{ijk} = \mathbb{Q}_{n,ijk}V_{ijk} . \tag{82}$$

Discretizing Fick's Law gives

$$\begin{aligned} \mathbb{J}_{n,l+1/2} &= -\frac{1}{\Delta_{l+1/2}}\mathbb{D}_{n,l+1/2}(\mathbb{U}_{n,l+1} - \mathbb{U}_{n,l}) , \\ \mathbb{J}_{n,l-1/2} &= -\frac{1}{\Delta_{l-1/2}}\mathbb{D}_{n,l-1/2}(\mathbb{U}_{n,l} - \mathbb{U}_{n,l-1}) , \end{aligned} \tag{83}$$

Using the same technique to solve for the edge diffusion terms, but recognizing that these are $(N_g \times N_g)$ matrices in the multigroup problem, yields an analog to Eq. (57):

$$\begin{aligned}\frac{\mathbb{D}_{n,l+1/2}}{\Delta_{l+1/2}}(\mathbb{U}_{n,l+1}-\mathbb{U}_{n,l}) &= 2\mathbb{D}_{n,l+1}(\Delta_l\mathbb{D}_{n,l+1}+\Delta_{l+1}\mathbb{D}_{n,l})^{-1}\mathbb{D}_{n,l}(\mathbb{U}_{n,l+1}-\mathbb{U}_{n,l})\,,\\ \frac{\mathbb{D}_{n,l-1/2}}{\Delta_{l-1/2}}(\mathbb{U}_{n,l}-\mathbb{U}_{n,l-1}) &= 2\mathbb{D}_{n,l}(\Delta_l\mathbb{D}_{n,l-1}+\Delta_{l-1}\mathbb{D}_{n,l})^{-1}\mathbb{D}_{n,l-1}(\mathbb{U}_{n,l}-\mathbb{U}_{n,l-1})\,.\end{aligned} \tag{84}$$

Applying these terms in Eq. (82) and (83) gives the multigroup analog to Eq. (58):

$$\begin{aligned}&-\mathbb{C}^+_{n,i}\mathbb{U}_{n,i+1\,jk}-\mathbb{C}^-_{n,i}\mathbb{U}_{n,i-1\,jk}-\mathbb{C}^+_{n,j}\mathbb{U}_{n,i\,j+1\,k}-\mathbb{C}^-_{n,j}\mathbb{U}_{n,i\,j-1\,k}-\mathbb{C}^+_{n,k}\mathbb{U}_{n,ij\,k+1}-\mathbb{C}^-_{n,k}\mathbb{U}_{n,ij\,k-1}-\\ &\sum_{m=1}^{4}\left[\mathbb{A}_{nm,ijk}+(\mathbb{C}^+_{m,i}+\mathbb{C}^-_{m,i}+\mathbb{C}^+_{m,j}+\mathbb{C}^-_{m,j}+\mathbb{C}^+_{m,k}+\mathbb{C}^-_{m,k})\delta_{nm}\right]\mathbb{U}_{m,ijk}=\mathbb{Q}_{n,ijk}\,,\quad n=1,2,3,4\,,\end{aligned} \tag{85}$$

where

$$\begin{aligned}\mathbb{C}^+_{n,l} &= \frac{2}{\Delta_l}\mathbb{D}_{n,l+1}(\Delta_l\mathbb{D}_{n,l+1}+\Delta_{l+1}\mathbb{D}_{n,l})^{-1}\mathbb{D}_{n,l}\,,\\ \mathbb{C}^-_{n,l} &= \frac{2}{\Delta_l}\mathbb{D}_{n,l}(\Delta_l\mathbb{D}_{n,l-1}+\Delta_{l-1}\mathbb{D}_{n,l})^{-1}\mathbb{D}_{n,l-1}\,,\\ l &= i,j,k\,.\end{aligned} \tag{86}$$

Recall that all terms in $\mathbb{A}$ notation are N_g-dimensioned matrices or vectors. Thus, we have

$$(N_g \times N_g)(N_g \times 1) = (N_g \times 1)\,.$$

The multigroup Marshak boundary conditions, following Eq. (38) are

$$-\hat{\mathbf{n}}\cdot\mathbb{J}_n+\sum_{m=1}^{4}\mathbb{B}_{nm}\mathbb{U}_m=\mathbb{S}_n\,, \tag{87}$$

where the $\mathbb{B}_{nm}$ are $(N_g \times N_g)$ diagonal matrices with B_{nm} from Eq. (40) on the diagonal and,

$$\mathbf{s}=\begin{pmatrix}\phi^0_{\rm b} & \phi^1_{\rm b} & \ldots & \phi^G_{\rm b}\end{pmatrix}^T\,, \tag{88}$$

and

$$\mathbb{S}_1=\frac{1}{2}\mathbf{s}\,,\quad \mathbb{S}_2=-\frac{1}{8}\mathbf{s}\,,\quad \mathbb{S}_3=\frac{1}{16}\mathbf{s}\,,\quad \mathbb{S}_4=-\frac{5}{128}\mathbf{s}\,. \tag{89}$$

Following the process that lead to Eqs. (65) and (66) using the multigroup formulation gives

$$\sum_{m=1}^{4}\left(\mathbb{B}_{nm}+\frac{2}{\Delta_1}\mathbb{D}_{n,1}\delta_{nm}\right)\mathbb{U}_{m,1/2}-\frac{2}{\Delta_1}\mathbb{D}_{n,1}\mathbb{U}_{n,1}=\mathbb{S}_n\,,\qquad \text{Low Boundary}\,, \tag{90}$$

$$\sum_{m=1}^{4}\left(\mathbb{B}_{nm}+\frac{2}{\Delta_L}\mathbb{D}_{n,L}\delta_{nm}\right)\mathbb{U}_{m,L+1/2}-\frac{2}{\Delta_L}\mathbb{D}_{n,L}\mathbb{U}_{n,L}=\mathbb{S}_n\,,\qquad \text{High Boundary}\,. \tag{91}$$

At the problem boundaries, the following equations provide the edge currents in Eq. (82)

$$\mathbb{J}_{n,1/2}=-\frac{2}{\Delta_1}\mathbb{D}_{n,1}(\mathbb{U}_{n,1}-\mathbb{U}_{n,1/2})\,,\qquad \text{Low Boundary}\,, \tag{92}$$

$$\mathbb{J}_{n,L+1/2}=-\frac{2}{\Delta_L}\mathbb{D}_{n,L}(\mathbb{U}_{n,L+1/2}-\mathbb{U}_{n,L})\,,\qquad \text{High Boundary}\,. \tag{93}$$

Likewise, reflecting boundary conditions are imposed in the following:

$$\mathbb{J}_{n,1/2} = 0\,, \qquad \text{Low Boundary}\,, \tag{94}$$

$$\mathbb{J}_{n,L+1/2} = 0\,, \qquad \text{High Boundary}\,, \tag{95}$$

which get used in Eq. (85) at reflecting boundaries.

Applying these conditions at the boundaries gives

$$\begin{aligned} \mathbb{C}^{-}_{n,1} &= \frac{2}{\Delta_1^2}\mathbb{D}_{n,1}\,, \quad \text{Low Boundary}\,, \\ \mathbb{C}^{+}_{n,L} &= \frac{2}{\Delta_l^2}\mathbb{D}_{n,L}\,, \quad \text{High Boundary}\,, \\ l &= i,j,k\,. \end{aligned} \tag{96}$$

where $\mathbb{U}_{n,l-1} \to \mathbb{U}_{n,1/2}$ and $\mathbb{U}_{n,l+1} \to \mathbb{U}_{n,L+1/2}$ at the low and high boundaries, respectively. Equations (90) and (91) provide the additional equations for the the edge fluxes and are used to close the system. On reflecting boundaries we have

$$\begin{aligned} \mathbb{C}^{-}_{n,1} &= 0\,, \qquad \text{Low Boundary}\,, \\ \mathbb{C}^{+}_{n,L} &= 0\,, \qquad \text{High Boundary}\,, \\ l &= i,j,k\,. \end{aligned} \tag{97}$$

No additional equations are required to close the system because the edge fluxes vanish.

6 Eigenvalue Form

The eigenvalue form of the 1-D transport equation, Eq. (69), is

$$\mu\frac{\partial\psi^g(x,\mu)}{\partial x} + \sigma^g(x)\psi^g(x,\mu) = \sum_{g'=0}^{G}\int_{4\pi}\sigma_{\rm s}^{gg'}(x,\hat{\mathbf{\Omega}}\cdot\hat{\mathbf{\Omega}}')\psi^{g'}(x,\mathbf{\Omega}')\,d\mathbf{\Omega}' + \frac{1}{k}\sum_{g'=0}^{G}\frac{\chi^g}{4\pi}\int_{4\pi}\nu\sigma_{\rm f}^{g'}(x)\,\psi^{g'}(x,\mathbf{\Omega}')\,d\mathbf{\Omega}'\,. \tag{98}$$

Expanding the eigenvalue term using the Eq. (3) and applying the orthogonalization property in Eq. (5) yields

$$\begin{aligned} \frac{1}{k}\sum_{g'=0}^{G}\frac{\chi^g}{4\pi}\int_{4\pi}\nu\sigma_{\rm f}^{g'}(x)\,\psi^{g'}(x,\mathbf{\Omega}')\,d\mathbf{\Omega}' &= \frac{1}{k}\sum_{g'=0}^{G}\frac{\chi^g}{2}\int_{-1}^{1}\nu\sigma_{\rm f}^{g'}\left[\sum_n\frac{2n+1}{4\pi}\phi_n P_n(\mu)\right]d\mu' \\ &= \frac{1}{k}\sum_{g'=0}^{G}\frac{\chi^g}{4\pi}\nu\sigma_{\rm f}^{g'}\,\phi_n^{g'}\delta_{n0}\,. \end{aligned} \tag{99}$$

The eigenvalue form of the P_N equations proceeds by using this term for the source term in Eq. (10). Applying the SP_N approximation described in §§ 3 and 5 to the resulting multigroup, eigenvalue P_N equations gives

$$\begin{aligned} -\frac{\partial}{\partial x_i}\Bigg[\frac{n}{2n+1}(\mathbf{\Sigma}_{n-1}^{-1})\frac{\partial}{\partial x_i}\Big(\frac{n-1}{2n-1}\Phi_{n-2}+\frac{n}{2n-1}\Phi_n\Big)+ \\ \frac{n+1}{2n+1}(\mathbf{\Sigma}_{n+1}^{-1})\frac{\partial}{\partial x_i}\Big(\frac{n+1}{2n+3}\Phi_n+\frac{n+2}{2n+3}\Phi_{n+2}\Big)\Bigg]+ \\ \mathbf{\Sigma}_n\Phi_n = \frac{1}{k}\mathbf{F}\Phi_n\delta_{n0}\,, \quad m=0,2,\ldots,N\,. \end{aligned} \tag{100}$$

The fission matrix, $\mathbf{F}$ is defined

$$\mathbf{F} = \begin{pmatrix} \chi^0 \nu\sigma_{\rm f}^0 & \chi^0 \nu\sigma_{\rm f}^1 & \dots & \chi^0 \nu\sigma_{\rm f}^G \\ \chi^1 \nu\sigma_{\rm f}^0 & \chi^1 \nu\sigma_{\rm f}^1 & \dots & \chi^1 \nu\sigma_{\rm f}^G \\ \vdots & \vdots & \ddots & \vdots \\ \chi^G \nu\sigma_{\rm f}^0 & \chi^G \nu\sigma_{\rm f}^1 & \dots & \chi^G \nu\sigma_{\rm f}^G \end{pmatrix} . \tag{101}$$

Converting the state unknowns from $\Phi \to \mathbb{U}$ via Eq. (77) gives the following eigensystem,

$$-\nabla \cdot \mathbb{D}_n \nabla \mathbb{U}_n + \sum_{m=1}^{4} \mathbb{A}_{nm} \mathbb{U}_m = \frac{1}{k} \sum_{m=1}^{4} \mathbb{F}_{nm} \mathbb{U}_{nm} \,, \quad n = 1, 2, 3, 4 \,, \tag{102}$$

where

$$\mathbb{F} = \begin{pmatrix} \mathbf{F} & -\frac{2}{3}\mathbf{F} & \frac{8}{15}\mathbf{F} & -\frac{16}{35}\mathbf{F} \\ -\frac{2}{3}\mathbf{F} & \frac{4}{9}\mathbf{F} & -\frac{16}{45}\mathbf{F} & \frac{32}{105}\mathbf{F} \\ \frac{8}{15}\mathbf{F} & -\frac{16}{45}\mathbf{F} & \frac{64}{225}\mathbf{F} & -\frac{128}{525}\mathbf{F} \\ -\frac{16}{35}\mathbf{F} & \frac{32}{105}\mathbf{F} & -\frac{128}{525}\mathbf{F} & \frac{256}{1225}\mathbf{F} \end{pmatrix} . \tag{103}$$

7 Adjoint Form

The adjoint form of the 1-D transport equation, Eq. (69), is

$$-\mu \frac{\partial \psi^{\dagger\, g}(x,\mu)}{\partial x} + \sigma^g(x) \psi^{\dagger\, g}(x,\mu) = \sum_{g'=0}^{G} \int_{4\pi} \sigma_{\rm s}^{g'\, g}(x, \hat{\mathbf{\Omega}} \cdot \hat{\mathbf{\Omega}}') \psi^{\dagger\, g'}(x, \mathbf{\Omega}')\, d\mathbf{\Omega}' + \frac{q^{\dagger\, g}(x)}{4\pi} \,, \tag{104}$$

where $\psi^{\dagger\, g}$ is the adjoint flux for group g. Likewise, the adjoint form of Eq. (98) is

$$\begin{aligned} -\mu \frac{\partial \psi^{\dagger\, g}(x,\mu)}{\partial x} + \sigma^g(x) \psi^{\dagger\, g}(x,\mu) = \\ \sum_{g'=0}^{G} \int_{4\pi} \sigma_{\rm s}^{g'\, g}(x, \hat{\mathbf{\Omega}} \cdot \hat{\mathbf{\Omega}}') \psi^{\dagger\, g'}(x, \mathbf{\Omega}')\, d\mathbf{\Omega}' + \frac{1}{k^\dagger} \sum_{g'=0}^{G} \frac{\chi^{g'}}{4\pi} \int_{4\pi} \nu\sigma_{\rm f}^g(x)\, \psi^{\dagger\, g'}(x, \mathbf{\Omega}')\, d\mathbf{\Omega}' \,. \end{aligned} \tag{105}$$

Applying the P_N approximation to Eq. (104) gives

$$-\frac{\partial}{\partial x}\Big[\frac{n}{2n+1}\phi_{n-1}^{\dagger\, g} + \frac{n+1}{2n+1}\phi_{n+1}^{\dagger\, g}\Big] + \sum_{g'} (\sigma^g \delta_{gg'} - \sigma_{{\rm s}n}^{g'\, g}) \phi_n^{\dagger\, g'} = q^{\dagger\, g} \delta_{n0} \,, \quad n = 0, 1, 2, \dots, N \,. \tag{106}$$

Following the steps in §§ 3 and 5, the adjoint SP_N equations are

$$-\frac{\partial}{\partial x_i}\Big[\frac{n}{2n+1}\phi_{n-1,i}^{\dagger\, g} + \frac{n+1}{2n+1}\phi_{n+1,i}^{\dagger\, g}\Big] + \sum_{g'} (\sigma^g \delta_{gg'} - \sigma_{{\rm s}n}^{g'\, g}) \phi_n^{\dagger\, g'} = q^{\dagger\, g} \delta_{n0} \,, \qquad n = 0, 2, 4, \dots, N \,, \tag{107}$$

$$-\frac{\partial}{\partial x_i}\Big[\frac{n}{2n+1}\phi_{n-1}^{\dagger\, g} + \frac{n+1}{2n+1}\phi_{n+1}^{\dagger\, g}\Big] + \sum_{g'} (\sigma^g \delta_{gg'} - \sigma_{{\rm s}n}^{g'\, g}) \phi_{n,i}^{\dagger\, g'} = 0 \,, \qquad n = 1, 3, 5, \dots, N \,. \tag{108}$$

Using Eq. (108) to solve for the $\phi^{\dagger\, g}_{n,i}$ terms and substituting into Eq. (108) gives

$$-\frac{\partial}{\partial x_i}\left[\frac{n}{2n+1}(\mathbf{\Sigma}^\dagger_{n-1})^{-1}\frac{\partial}{\partial x_i}\left(\frac{n-1}{2n-1}\Phi^\dagger_{n-2}+\frac{n}{2n-1}\Phi^\dagger_n\right)+\right.$$
$$\left.\frac{n+1}{2n+1}(\mathbf{\Sigma}^\dagger_{n+1})^{-1}\frac{\partial}{\partial x_i}\left(\frac{n+1}{2n+3}\Phi^\dagger_n+\frac{n+2}{2n+3}\Phi^\dagger_{n+2}\right)\right]+$$
$$\mathbf{\Sigma}^\dagger_n\Phi^\dagger_n=\mathbf{q}^\dagger\delta_{n0}\,,\quad m=0,2,\ldots,N\,, \tag{109}$$

where

$$\Phi^\dagger_n=\begin{pmatrix}\phi^{\dagger\,0}_n & \phi^{\dagger\,1}_n & \ldots & \phi^{\dagger\,G}_n\end{pmatrix}^T\,, \tag{110}$$

$$\Phi^\dagger_{n,i}=\begin{pmatrix}\phi^{\dagger\,0}_{n,i} & \phi^{\dagger\,1}_{n,i} & \ldots & \phi^{\dagger\,G}_{n,i}\end{pmatrix}^T\,, \tag{111}$$

$$\mathbf{q}^\dagger=\begin{pmatrix}q^{\dagger\,0} & q^{\dagger\,1} & \ldots & q^{\dagger\,G}\end{pmatrix}^T\,, \tag{112}$$

and

$$\mathbf{\Sigma}^\dagger_n=\begin{pmatrix}(\sigma^0-\sigma^{00}_{sn}) & -\sigma^{10}_{sn} & \ldots & -\sigma^{G0}_{sn}\\ -\sigma^{01}_{sn} & (\sigma^1-\sigma^{11}_{sn}) & \ldots & -\sigma^{G1}_{sn}\\ \vdots & \vdots & \ddots & \vdots\\ -\sigma^{0G}_{sn} & -\sigma^{1G}_{sn} & \ldots & (\sigma^G-\sigma^{GG}_{sn})\end{pmatrix}\,. \tag{113}$$

Equations (109) through (113) constitute the adjoint, multigroup SP_N equations.

Equation (109) is identical in form to Eq. (76); thus, all of the machinery that was derived to solve the multigroup SP_N equations in § 5, starting with Eq. (77), can be used to solve the adjoint SP_N equations. The only requirements to convert the forward solver to an adjoint solver are:

1. use an adjoint external source (response)
2. take the transpose of the all of the cross section matrices because

$$\mathbf{\Sigma}^\dagger_n=\mathbf{\Sigma}^T_n\,. \tag{114}$$

For eigenvalue equations the fission matrix must be transposed as well because $\mathbf{F}^\dagger=\mathbf{F}^T$,

$$\mathbf{F}^\dagger=\begin{pmatrix}\chi^0\nu\sigma^0_f & \chi^1\nu\sigma^0_f & \ldots & \chi^G\nu\sigma^0_f\\ \chi^0\nu\sigma^1_f & \chi^1\nu\sigma^1_f & \ldots & \chi^G\nu\sigma^1_f\\ \vdots & \vdots & \ddots & \vdots\\ \chi^0\nu\sigma^G_f & \chi^1\nu\sigma^G_f & \ldots & \chi^G\nu\sigma^G_f\end{pmatrix}\,. \tag{115}$$

All other aspects of solving the adjoint eigenvalue form of the SP_N equations follows from § 6.

8 Matrix System

The multigroup SP_N equations have dimension $N_g\times N_m\times N_c$ where $N_m=(N+1)/2$ is the number of moment equations and N_c is the number of spatial cells. The solution vector $\mathbf{u}$ can be ordered in multiple

ways. As we shall show, the ordering that minimizes the bandwidth of the matrix is to order $\mathbf{u}$ in groups-moments-cells,

$$\mathbf{u} = \begin{pmatrix} u_0 & u_1 & \dots & u_{m-1} & u_m & u_{m+1} & \dots & u_M \end{pmatrix}^T , \tag{116}$$

with

$$m = g + N_g(n + cN_m) , \tag{117}$$

where g is the group, n is the moment-equation, and c is the cell.

The matrix system described in Eq. (85) is

$$\mathbf{A}\mathbf{u} = \mathbf{Q} . \tag{118}$$

Consider an example SP_3 matrix that results from a $4 \times 4 \times 4$ grid with 2 groups and all reflecting boundary conditions. The total number of unknowns is 256. There 4 equations in cell 0,

$$\begin{aligned}(A^{00}_{00,0} + C^{+00}_{0,0} + C^{+00}_{0,0} + C^{+00}_{0,0})u_0 + (A^{01}_{00,0} + C^{+01}_{0,0} + C^{+01}_{0,0} + C^{+01}_{0,0})u_1 + A^{00}_{01,0}u_2 + A^{01}_{01,0}u_3 \\ - C^{+00}_{0,0}u_4 - C^{+01}_{0,0}u_5 - C^{+00}_{0,0}u_{16} - C^{+01}_{0,0}u_{17} - C^{+00}_{0,0}u_{64} - C^{+01}_{0,0}u_{65} = q^0_0\end{aligned} \tag{119a}$$

$$\begin{aligned}(A^{10}_{00,0} + C^{+10}_{0,0} + C^{+10}_{0,0} + C^{+10}_{0,0})u_0 + (A^{11}_{00,0} + C^{+11}_{0,0} + C^{+11}_{0,0} + C^{+11}_{0,0})u_1 + A^{10}_{01,0}u_2 + A^{11}_{01,0}u_3 \\ - C^{+10}_{0,0}u_4 - C^{+11}_{0,0}u_5 - C^{+10}_{0,0}u_{16} - C^{+11}_{0,0}u_{17} - C^{+10}_{0,0}u_{64} - C^{+11}_{0,0}u_{65} = q^1_0\end{aligned} \tag{119b}$$

$$\begin{aligned}A^{00}_{10,0}u_0 + A^{01}_{10,0}u_1 + (A^{00}_{11,0} + C^{+00}_{1,0} + C^{+00}_{1,0} + C^{+00}_{1,0})u_2 + (A^{01}_{11,0} + C^{+01}_{1,0} + C^{+01}_{1,0} + C^{+01}_{1,0})u_3 \\ - C^{+00}_{1,0}u_6 - C^{+01}_{1,0}u_7 - C^{+00}_{1,0}u_{18} - C^{+01}_{1,0}u_{19} - C^{+00}_{1,0}u_{66} - C^{+01}_{1,0}u_{67} = -\frac{2}{3}q^0_0\end{aligned} \tag{119c}$$

$$\begin{aligned}A^{10}_{10,0}u_0 + A^{11}_{10,0}u_1 + (A^{10}_{11,0} + C^{+10}_{1,0} + C^{+10}_{1,0} + C^{+10}_{1,0})u_2 + (A^{11}_{11,0} + C^{+11}_{1,0} + C^{+11}_{1,0} + C^{+11}_{1,0})u_3 \\ - C^{+10}_{1,0}u_6 - C^{+11}_{1,0}u_7 - C^{+10}_{1,0}u_{18} - C^{+11}_{1,0}u_{19} - C^{+10}_{1,0}u_{66} - C^{+11}_{1,0}u_{67} = -\frac{2}{3}q^1_0\end{aligned} \tag{119d}$$

Vacuum and source boundary conditions must be coupled over all equations as indicated by Eq. (87); thus the size of the matrix will be augmented by $N_b \times N_g \times N_m$ unknowns where N_b is the number of boundary cells over all faces. The sparsity plot for a $4 \times 4 \times 4$ grid with isotropic flux boundary conditions on each face is shown in Fig. 4

References

[1] E. Gelbard, "Application of the spherical harmonics to reactor problems," Tech. Rep. WAPD-BT-20, Westinghouse Atomic Power Department, Sept 1960.

[2] M. Frank, A. Klar, E. W. Larsen, and S. Yasuda, "Time-dependent simplified PN approximation to the equations of radiative transfer," *Journal of Computational Physics*, vol. 226, pp. 2289–2305, Oct. 2007.

[3] E. W. Larsen, G. Thömmes, A. Klar, M. Sead, and T. Götz, "Simplified PN Approximations to the Equations of Radiative Heat Transfer and Applications," *Journal of Computational Physics*, vol. 183, pp. 652–675, Dec. 2002.

[4] E. W. Larsen, J. E. Morel, and J. M. McGhee, "Asymptotic Derivation of the Multigroup P1 and Simplified PN Equations with Anisotropic Scattering," *Nuclear Science and Engineering*, vol. 123, pp. 328–342, 1996.

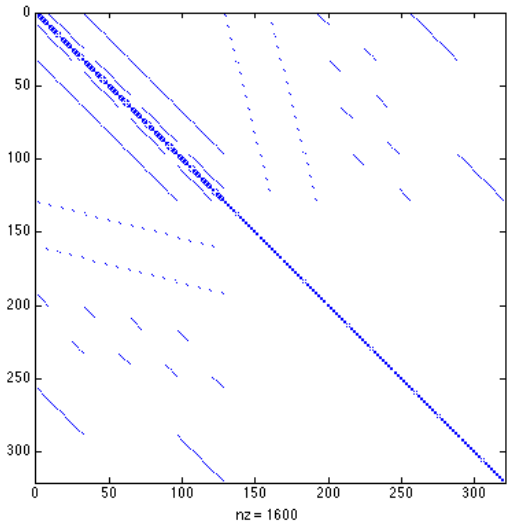

Figure 4: SP_3 matrix sparsity pattern.

[5] P. S. Brantley and E. W. Larsen, "The Simplified P3 Approximation," *Nuclear Science and Engineering*, vol. 134, pp. 1–21, 2000.

[6] A. D. Klose and E. W. Larsen, "Light transport in biological tissue based on the simplified spherical harmonics equations," *Journal of Computational Physics*, vol. 220, pp. 441–470, Dec. 2006.

[7] T. Evans, A. Stafford, R. Slaybaugh, and K. Clarno, "DENOVO: A new three-dimensional parallel discrete ordinates code in SCALE," *Nuclear Technology*, vol. 171, pp. 171–200, 2010.

Distribution

9te <9te@ornl.gov>

CAUTION

This document has not been given final patent clearance and is for internal use only. If this document is to be given public release, it must be cleared through the site Technical Information Office, which will see that the proper patent and technical information reviews are completed in accordance with the policies of Oak Ridge National Laboratory and UT-Battelle, LLC.